

奈米碳材料的合成及電化學電容器之應用

學生：洪淙琦

指導教授：陳家富 博士

黃華宗 博士

國立交通大學材料科學與工程學系（研究所）博士班

摘要

奈米碳管具有優異且獨特的化學與物理特性，應用於各種領域深具有淺力，例如場發射顯示器、儲氫材料、能量儲存、奈米電子元件及複合材料等。奈米碳管主要的合成法包括：雷射蒸發法、電弧法以及化學氣相沈積法，作為觸媒之用的過渡金屬（鐵、鈷、鎳）對於採用化學氣相沈積法尤其重要。

本研究論文採用偏壓輔助微波電漿化學沈積系統合成多種結晶性奈米碳材料於碳布以及不鏽鋼片上，包括垂直以及交錯成長的奈米碳管、接合奈米碳薄片的奈米碳管以及二維和三維結構的奈米碳薄片，這多樣的奈米碳結構可以經由通入不同的氣氛系統而達到，包含了甲烷/氫氣以及甲烷/二氧化碳系統；甲烷/氫氣(1:4)的系統可用作在含有鐵觸媒的基板上成長純奈米碳管的前驅物氣體來源。當中，交錯成長的奈米碳管是在沒有施加外部偏壓的情況下可以得到，而垂直成長的奈米碳管則是藉由施加相對於在系統上電極的-150 伏特偏壓而得到，除此之外，有趣的是，接合奈米碳薄片的碳管也可以藉由相同的系統得到，只是鍍有鐵觸媒的基材在氫氣的氣氛下需先經過 400°C 退火 5 小時，類似的接合結構也可以在不鏽鋼基材上藉由甲烷/二氧化碳(3:2) 的系統得到，同樣地考慮施加偏壓，這樣的接合結構只有在施加-150 伏特偏壓 的情形下才能達到，相較之下，在不施加偏壓以及-100 伏特的情形下會得到奈米碳薄片以及球狀奈米碳薄片的結構；在相同的甲烷/二氧化碳系統之下，我們利用沒有觸媒的沈積方式，藉由碳原子間碰撞的原理，可以在碳布上得到二維的碳薄片結構，在不用觸媒的考慮下，我們也嘗試著將二維的結構轉為三維的堆疊，利用醋酸在 90°C 下進酸化 6 個小時，便可以在原本的二維結構上繼續碳的沈積以轉變為具有花簇狀碳薄片的第二層堆疊。這

些碳結構則是藉由掃描式、穿透式電子顯微鏡、拉曼光譜儀以及 X 光繞射儀進行量測。

論文的第二部份則事先藉由不同濃度的醋酸(2M 及 14M)在 90°C 以及不同的時間條件下對垂直成長的奈米碳管進行酸化以探究官能基的數量極限，我們發現官能基的數量極限在 2M 以及 14M 的條件下分別可以在 12 小時以及 6 小時得到。應用在超高電容器上，有著奈米碳薄片接合的碳管，其電容量則會有效的提昇，可以達到將近 194 F/g，幾乎是純碳管電極的兩倍;在不用觸媒沈積的碳薄片方面，三維碳薄片結構的電極顯示出較二維碳薄片結構近四倍大的電容量，這主要是因為孔洞的尺寸分佈趨近於 3 nm，這樣的結果是有利於電荷的儲存;在本論文研究中，所有的含碳結構的電極其循環效率在經過 2000 次的循環之後都還可以超過 90%，我們認為含有奈米碳薄片的碳結構也許在能量儲存系統的應用上可以提供一個另外的選擇，尤其是在電化學電容器上。



Synthesis of Carbon Nanomaterials and Applications on Electrochemical Capacitor

Student : Tsung-Chi Hung

Advisor : Dr. Chia-Fu Chen

Dr. Wha-Tzong Whang

Department of Materials Science and Engineering

National Chiao Tung University

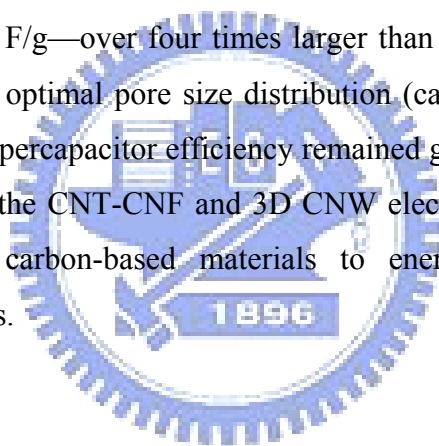
Abstract

Carbon nanotubes (CNTs) have unique properties that make them suitable for use in various applications, such as field emission displays, energy storage, chemical sensors, nano-electronic devices, and composite materials. The available methods for synthesizing CNTs include arc-discharging, laser vaporization, and chemical vapor deposition using transition metals (e.g., Fe, Co, Ni) as catalysts.

In the studies reported in this Thesis, we used a bias-assisted microwave plasma-enhanced chemical vapor deposition (MPCVD) system to synthesize various crystalline carbon nanomaterials, including aligned and interlaced CNTs, CNTs decorated with carbon nanowalls (CNWs), and two- and three-dimensional CNWs on carbon cloth (CC) and stainless-steel (SS) substrates. The nature of the resulting carbon structures varied depending on the choice of the gaseous system (CH_4/H_2 , CH_4/CO_2). The CH_4/H_2 system at a ratio of 1:4 served as a precursor for the synthesis of pure CNTs on both the CC and SS substrates, with Fe as the catalyst. Interlaced CNTs formed in the absence of an applied external bias; aligned CNTs formed when applying an external bias of at least -150 V with respect to the upper electrode in the MPCVD system. Interestingly, CNTs decorated with CNWs on their surfaces were synthesized on the Fe-coated CC subjected to annealing under a N_2 atmosphere at 400 °C for 5 h; an analogous structure was formed on the SS substrate when introducing the mixture of CH_4 and CO_2 at a specific flow ratio of 3:2. CNTs decorated with CNWs were obtained when applying a negative bias of -150 V, whereas CNW sheets and spherical CNWs resulted at biases of 0 and -100 V, respectively. In the same CH_4/CO_2 system, but without any added catalyst, normal 2D CNWs were formed on the CC substrate through the collision of carbon atoms. Using catalyst-free conditions, we turned these 2D structures into 3D

constructions by stacking flower-like aggregates of CNWs onto the 2D sheets, which had been functionalized under the influence of HNO_3 at ca. $90\text{ }^\circ\text{C}$ for 6 h. The structures were characterized using scanning electron microscopy (SEM), transmission electron microscopy (TEM), Raman spectroscopy, and X-ray diffraction (XRD).

The second part of this Thesis describes the quantitative limitations of the number of functional groups that could be formed on aligned CNTs after oxidizing them with various concentrations of HNO_3 at $90\text{ }^\circ\text{C}$ for various periods of time. Using 2 and 14 M HNO_3 , the maximum number of functional groups was obtained after 12 and 6 h, respectively, as measured in terms of quantity of Pt particles. Subsequently, the different kinds of carbon materials described in this Thesis were functionalized with 14 M HNO_3 over 6 h to test their applicability for use as supercapacitors. The capacitance was increased dramatically to ca. 194 F/g after attaching the CNWs to the CNTs, almost doubling the value of the electrode formed from pure CNTs (ca. 100 F/g). The 3D construction of CNWs exhibited an enormous increase in capacitance to ca. 200 F/g—over four times larger than that of the 2D sheets of the pure CNWs—because of their optimal pore size distribution (ca. 3 nm). For all of the electrodes tested in this study, the supercapacitor efficiency remained greater than 90% after 2000 cycles. The unique structures of the CNT-CNF and 3D CNW electrodes may provide another route for the application of carbon-based materials to energy storage systems, especially electrochemical capacitors.



致謝

本論文能順利完成，首先要感謝我的指導教授陳家富/黃華宗老師在論文研究上的指導與鼓勵，更重要的是陳老師及黃老師對學生的照顧及愛護，讓我得以順利完成學業，開拓未來更寬廣的道路。感謝論文審查委員對於本論文的指導及提供寶貴的建議，在此由衷表示感謝。

感謝實驗室同仁陳密學姐、林建良學長、施士塵學長、陳建仲學長、徐振航學長、羅鴻鈞學長、劉厥楊學長、施騰凱學長等在研究上提供的建議及協助，感謝王瑞豪同學、羅俊傑學弟在研究上熱情相助，另外也感謝羅傑、小白、阿村、嘉忻、小卓、建諳、阿炮在生活中讓我留下許多美好的回憶。

同時也感謝國科會在經費上得補助，國家奈米實驗室及交大奈米中心在分析設備上的支持。

最後，我要感謝家人爸爸、媽媽、佑國、瑜筑、曉青的支持鼓勵與陪伴，感謝媽媽的一席話。僅以此論文獻給我最愛的家人與已逝的奶奶。



Contents

Abstract(Chinese)	i
Abstract(English)	iii
Acknowledgement	v
Contents	vi
Table Captions	vi
Figure Captions	vii
Chapter 1	Introduction.....	1
1.1	Carbon nanomaterials.....	1
1.1.1	Carbon nanotubes (CNTs).....	2
1.1.1.1	Structures and properties of CNTs.....	3
1.1.1.1.1	Structures of CNTs.....	3
1.1.1.1.2	Electronic properties of CNTs.....	6
1.1.1.1.3	Mechanical properties of CNTs.....	8
1.1.2	Carbon nanowalls (CNWs).....	9
1.1.2.1	Structures and properties of CNWs.....	9
1.1.2.1.1	Structures of CNWs.....	10
1.1.2.1.2	Properties of CNWs.....	11
1.1.3	Application of carbon nanomaterials.....	12
1.1.3.1	Energy storage.....	12
1.1.3.2	Supercapacitors.....	12
1.1.3.3	Hydrogen storage.....	13
1.1.3.4	Lithium intercalation.....	13
1.1.3.5	Field emission devices.....	14
1.1.3.6	Composite materials.....	14
1.1.3.7	Transistors.....	15
1.1.3.8	Templates.....	16
1.1.3.9	Nanoprobes and sensors.....	16
1.1.4	Carbon nanomaterial synthesis.....	17
1.1.4.1	Arc discharging.....	18
1.1.4.2	Laser ablation.....	19

1.1.4.3	Catalyst chemical vapor deposition.....	20
1.1.4.4	Catalytic growth mechanisms of CNTs.....	24
1.2	Electrochemical capacitors.....	27
1.2.1	Faradaic and non-faradaic processes.....	30
1.2.1.1	Non-faradaic process.....	30
1.2.1.2	Faradaic process.....	30
1.2.2	Classification of electrochemical capacitors.....	31
1.2.2.1	Traditional capacitors.....	31
1.2.2.2	Electric double-layer capacitor.....	31
1.2.2.3	Pseudocapacitor.....	34
1.2.2.4	Conducting polymer capacitor.....	35
1.3	Motivation for this Thesis.....	35
Chapter 2	Literature Review.....	36
2.1	Purification of CNTs.....	36
2.1.1	Thermal oxidation.....	36
2.1.2	Microfiltration and ultrasonically assisted filtration.....	36
2.1.3	Acid treatment.....	37
2.1.4	Thermal oxidation combined with acid treatment.....	38
2.2	Fundamentals and structures of ECs.....	38
2.2.1	Principle of energy storage.....	40
2.2.2	Electrode material.....	42
2.2.2.1	Carbonaceous material.....	42
2.2.2.2	Metal oxides.....	44
2.2.2.3	Polymers.....	44
2.2.3	Electrolyte.....	45
2.2.3.1	Non-aqueous electrolytes.....	45
2.2.3.2	Aqueous electrolytes.....	46
2.3	Electrochemical characteristic of porous electrodes.....	47
Chapter 3	Experimental Details.....	52
3.1	Experimental flow chart for the growth and characterization of carbon nanomaterials.....	52
3.2	Deposition system: Bias-assisted MPCVD.....	53
3.3	Analytical instruments.....	55

3.3.1	XPS.....	55
3.3.2	Energy dispersive X-ray (EDX) analysis.....	55
3.3.3	SEM.....	56
3.3.4	TEM.....	57
3.3.5	Raman spectroscopy.....	58
3.3.6	XRD.....	58
3.3.7	Infrared (IR) spectroscopy.....	59
3.3.8	Cyclic voltammetry (CV).....	60
3.3.9	Brunauer–Emmit–Teller (BET) surface area.....	61
Chapter 4	Synthesis of Carbon Nanomaterials by MPCVD system.....	63
4.1	Synthesis of MWCNTs on carbon cloth and stainless steel.....	63
4.1.1	Sample preparation and experimental procedures.....	63
4.1.2	The effect of external bias on the formation of MWCNTs.....	63
4.1.3	Characteristics of the aligned MWCNTs.....	65
4.1.4	Summary.....	70
4.2	Synthesis of coral-like MWCNTs.....	71
4.2.1	Sample preparation and experimental procedures.....	71
4.2.2	Characteristics of the coral-like MWCNTs.....	72
4.2.3	Formation mechanisms of coral-like MWCNTs.....	81
4.2.4	Summary.....	83
4.3	Synthesis of graphitic CNWs on carbon cloth.....	84
4.3.1	Catalyst-free fabrication of 2-D and quasi-3-D CNWs electrode on carbon cloth.....	84
4.3.2	The effect of supplied power on the formation and properties of CNWs.....	85
4.3.3	Fabrication and characteristics of stacking 3-D CNWs.....	94
4.3.4	Formation mechanism of the stacking 3-D CNWs.....	101
4.3.5	Summary.....	102
Chapter 5	Electrochemical properties of carbon nanomaterials.....	103
5.1	Chemical treatment on carbon nanomaterials.....	103
5.1.1	Experimental procedures for acid treatment.....	103
5.1.2	Characteristics.....	104
5.1.2.1	FTIR and XPS measurements.....	104

5.1.2.2	Deposition of Pt on the MWCNTs.....	106
5.1.2.3	Quantitative limitation of active sites on carbon material.....	108
5.1.3	Summary.....	110
5.2	Electrochemical investigations of carbon nanomaterials.....	111
5.2.1	Aligned MWCNTs and coral-like CNTs in aqueous solution (H ₂ SO ₄ /H ₂ O).....	111
5.2.1.1	Experimental details.....	111
5.2.1.2	Electrochemical measurements.....	112
5.2.2	2-D and 3-D CNWs in aqueous solution (H ₂ SO ₄ /H ₂ O).....	116
5.2.2.1	Experimental details.....	116
5.2.2.2	Electrochemical measurements.....	117
5.2.3	Entangled MWCNTs and coral-like materials in non-aqueous electrolyte (GBL ion solution).....	119
5.2.3.1	Experimental details.....	119
5.2.3.2	Electrochemical measurements.....	119
5.2.4	Summary.....	125
Chapter 6	Conclusions.....	126
Reference	Reference.....	129

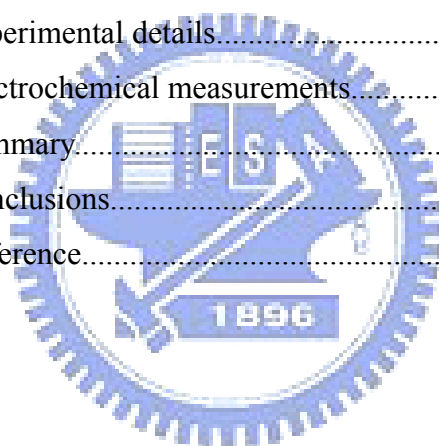


Table Captions

Table 1.1	Isomers of carbon.....	2
Table 1.2	Mechanical properties of CNTs compared with other Materials.....	9
Table 1.3	Metals and metal compounds catalysts for SWCNT synthesis.....	23
Table 1.4	Comparison of properties of secondary batteries and electrochemical capacitors.....	29
Table 1.5	Types of capacitors and mode of energy storage.....	32
Table 4.1	The quantitative properties of the CNWs electrodes synthesize at different power.....	94



Figure Captions

Figure 1.1	The three allotropes of carbon.....	2
Figure 1.2	Models of different CNT structures.....	4
Figure 1.3	Schematic diagram showing how a hexagonal sheet of graphite is rolled to form a CNT.....	5
Figure 1.4	TEM pictures of the ends of (a) a SWCNT, (b) a closed MWCNT, and (c) an open MWCNT. Each black line corresponds to one graphene sheet viewed edge-on.....	6
Figure 1.5	Schematic illustrations of CNWs synthesized vertically on the substrate.....	11
Figure 1.6	Schematic illustration of a CNW.....	11
Figure 1.7	A single semi-conducting nanotube is contacted by two electrodes. The Si substrate, which is covered by a layer of SiO ₂ 300nmthick, acts as a back-gate.....	16
Figure 1.8	Use of a MWNT as AFM tip. VGCF stands for Vapour Grown Carbon Fibre. At the centre of this fibre the MWNT forms the tip.....	17
Figure 1.9	Schematic illustration of the arc discharge system and TEM micrograph of the grown CNT.....	19
Figure 1.10	Schematic illustration of the laser ablation apparatus.....	20
Figure 1.11	Schematic illustration of the catalytic deposition and TEM micrograph of the grown CNT.....	21
Figure 1.12	Schematic diagram of vapor-solid (VS) growth model.....	25
Figure 1.13	Schematic diagram of VLS growth mechanism for nanotubes.....	26
Figure 1.14	Schematic depiction of SLS growth mechanism.....	26
Figure 1.15	Electric double layer capacitor constructed by inserting two electrodes in a beaker and applying a voltage. The voltage persists after the switch is opened (right), creating two series-connected capacitors. Charges in the electric double layer are separated by only about 1 nm.....	28
Figure 1.16	Representation of an electrolyte-filled right-cylindrical nanopore in a carbon electrode of an electrochemical capacitor showing the distributed resistance from the electrolyte and distributed charge storage down the interior surface of the nanopore.....	28
Figure 1.17	The sketch of electric double-layer capacitor in an aqueous electrolyte.....	33
Figure 2.1	Sketch of Ragone plot for various energy storage and conversion devices.....	39

Figure 2.2	schematic diagram of a double-layer structure.....	40
Figure 2.3	Illustration of the potential drop at the electrode/electrolyte interface.....	41
Figure 2.4	Cyclic voltammograms of activated glassy carbon electrodes at 100 mV/s in 3M H ₂ SO ₄ (aq.) and in 1 M TEABF ₄ in acetonitrile. Both electrodes received the same electrochemical activation.....	43
Figure 2.5	Equivalent circuit representation of the distributed resistance and capacitance within a pore. Five-element transmission line.....	50
Figure 2.6	Schematic representation of the Nyquist impedance plot of an ideal capacitor (vertical thin line) and an electrochemical capacitor with porous electrodes (thick line).....	50
Figure 2.7	Calculated impedance plots for porous electrodes with different thickness. Assumptions: Double layer capacitance: 10 μF/cm ² ; pore diameter: 3 nm; electrolyte conductivity 0.8 S/cm; rectangular closed packed arrangement of pores 10 ¹³ /cm ² ; constant phase element exponent 0.98.....	51
Figure 2.8	Capacitance versus frequency plot for the electrodes of Figure 2.7.....	51
Figure 2.9	Effect of pore diameter on the capacitance versus frequency performance of a single porous electrode. Thickness of porous layer: 100 μm, CPE: 0.98, double layer capacitance 20 μF, number of pores 2.5*10 ¹¹ /cm ²	51
Figure 3.1	Experiment flow chart of growth procedure and characterization of carbon nanomaterials.....	52
Figure 3.2	Bias- assisted microwave plasma-enhanced chemical vapor deposition system.....	54
Figure 3.3	Schematic diagram of a Scanning Electron Microscopy.....	56
Figure 3.4	Schematic diagram of a TEM.....	57
Figure 3.5	Schematic diagram of Raman spectroscopy.....	58
Figure 3.6	Schematic diagram of Bragg's law.....	59
Figure 3.7	A simple spectrometer layout.....	60
Figure 3.8	Schematic diagram of a cyclic voltammetry experiment.....	61
Figure 4.1	SEM image of the aligned MWCNTs synthesized on the Fe-coated carbon cloth substrate.....	64
Figure 4.2	SEM image of the entangled MWCNTs synthesized on the Fe-coated carbon cloth substrate.....	64
Figure 4.3	SEM image of the entangled MWCNTs synthesized on the stainless steel	

	substrate.....	65
Figure 4.4	Low-magnified SEM image of the aligned CNTs electrode.....	66
Figure 4.5	TEM images of (a) the aligned MWCNT (b) the entangled CNT synthesis on carbon cloth, (c) the entangled MWCNT on stainless steel plate, and (d) the EDX result of the catalyst encapsulated at the end of MWCNT of Figure 4.5(c).....	67
Figure 4.6	Raman shift spectra of (a) the aligned MWCNTs, (b) the entangled MWCNTs on carbon cloth, and (c) the MWCNTs on stainless steel plate.....	68
Figure 4.7	X-ray diffraction spectra of the electrodes containing (a) the aligned MWCNTs, (b) the entangled MWCNTs on carbon cloth, and (c) the MWCNTs on stainless steel plate (the peaks marked (*) refer to various phases of Al plate).....	69
Figure 4.8	SEM images of carbon materials prepared through MPCVD for 30 min. (a) CNTs-CNFs prepared in the absence of an applied external bias; (b) magnified image of the CNTs-CNFs electrode.....	73
Figure 4.9	TEM images of the (b) early and (c) late stages of development of CNFs attached to a CNT.....	74
Figure 4.10	The morphology of the SS substrate pretreated by hydrogen plasma at H ₂ flow of 10 sccm, power of 300 W, and pressure of 10 torr.....	76
Figure 4.11	Carbon nanomaterials prepared after performing bias-assisted MPCVD for 30 min: (a, b) pure CNFFs formed in the absence of an applied external bias; (c, d) CNFSs formed at an external applied bias of -100 V; (e, f) CNTs/CNFs formed at an external applied bias of -150 V.....	77
Figure 4.12	TEM images of (a) a CNT decorated with some CNFs, (b) a magnified CNT wall, (c) a CNT covered entirely by CNFs, and (d) top, (e) side views of a CNF/CNT structure and (f) the EDX measurement of the catalyst encapsulated at the end top of coral-like MWCNT.....	79
Figure 4.13	TEM images of a CNF attached to a CNT at the (a) beginning and (b) end of the formation process.....	80
Figure 4.14	Raman shift spectra of the coral-like CNTs synthesized on the Fe-coated carbon cloth (annealing at 400 °C) and stainless steel substrates.....	81
Figure 4.15	Schematic diagrams of the MWCNTs (a) decorated by CNWs through a peeling process by hydrogen termination and (b) The FTIR measurement.....	82

Figure 4.16	SEM images of (a) the flake-like carbon seeds synthesized on the carbon cloth for 5 min, and (b) deposition for 10 min and (c) for 15 min at 200 W; (d) at 300 W for 15 min; (e) at 400 W for 15 min and the inset of high-magnification image of tiny CNWs aggregation; (f) the quasi-3-D configuration of 400 W, with the H ₂ plasma pretreatment.....	87
Figure 4.17	SEM images of the deposition at 400 W (a) for 1 minute, (b) for 10 minutes, (c) for 30 minutes, and (d) the magnified image of the gathered structure in Figure 2(c).....	88
Figure 4.18	TEM images of (a) the carbon nanoflakes for 200 W, (b) for 300 W, and (c) for 400 W, with the H ₂ plasma pretreatment.....	89
Figure 4.19	SEM images of (a) the flake-like carbon seeds synthesized on the carbon cloth for 5 min, and (b) deposition for 10 min and (c) for 15 min at 200 W; (d) for 15 min at 300 W; (e) for 15 min at 400 W, without the H ₂ plasma pretreatment.....	91
Figure 4.20	The Raman measurement of (a) the carbon nanoflakes deposited at 200 W, 300 W, and 400 W with the H ₂ plasma pretreatment, and (b) without the H ₂ plasma pretreatment.....	92
Figure 4.21	The plots of the fraction I _D /I _G versus the applied power. ■ refers to the results with the H ₂ plasma pretreatment, and ▲ without the H ₂ plasma pretreatment.....	94
Figure 4.22	(a, b) SEM images of (a) the monolayer CNW film and (b) the double-layer CNWs at an early stage of deposition. (c) Low and (d) high magnification SEM images of the double-layer CNWs covering the as-grown CNW film, which was itself synthesized through MPCVD on carbon cloth (power: 300 W). (e) Pore size distribution of the double-layer electrode.....	98
Figure 4.23	TEM images of the flower-like CNWs: (a) low magnification of flower-like CNWs, and (b) graphite structure of the smallest CNWs.....	100
Figure 4.24	Schematic diagrams of the formation of double-layer CNWs structure: (a) Deposition of carbon atoms on the first 2D-CNWs layer; (b) nucleation; (c) aggregation of tiny CNWs; (d) formation of flower-like CNWs.....	101
Figure 5.1	TEM images of the MWNTs, synthesized by MPECVD, showed (a) before and (b) after the chemical oxidation (HNO ₃ , 14M).....	104
Figure 5.2	Infrared spectra of the electrodes treated in various periods of time (0 hr. ~	

	24 hr.) by (a) 2M and (b) 14M HNO ₃	105
Figure 5.3	C 1s spectrum of the HNO ₃ -MWNTs oxidized chemically at 90°C for 6hr (14M).....	106
Figure 5.4	The observation of strong Pt _{4f} peak of the XPS measurement.....	107
Figure 5.5	SEM images; (a) Pt nanoparticles on raw-MWNTs are agglomerated to be a larger nanoparticle and (b) Pt nanoparticles disperse uniformly on HNO ₃ -MWNTs.....	107
Figure 5.6	Function of the active surface area and Pt wt% as the period time of chemical oxidation (0 hr ~ 24 hours); (a) 2M, and (b) 14M.....	109
Figure 5.7	Cyclic voltammograms of (a) the well-aligned CNTs electrode and (b) the CNTs-CNWs electrode (electrolyte: 1 M H ₂ SO ₄ ; scan rates: 10, 50, 100, and 200 mV/s); (c) constant-current discharge diagrams of the well-aligned CNTs and CNTs-CNWs electrodes (constant discharge current: 1 mA).....	114
Figure 5.8	AC impedance plots (top) and fitting diagrams (bottom) for the (a) well-aligned CNTs and (b) CNTs-CNWs electrodes.....	115
Figure 5.9	Durability tests for the aligned CNTs and CNTs-CNWs electrodes; capacitance decay: ca. 9%.....	116
Figure 5.10	Cyclic voltammograms of (a) the double-layer CNWs electrode performed at different scan rates from 5 to 100 mV/s, and of the monolayer and double-layer CNWs electrodes performed at (b) 10 mV/s, (c) 50 mV/s, and (d) 100 mV/s. 1M H ₂ SO ₄ aqueous was used as the electrolyte.....	118
Figure 5.11	Cyclic voltammograms of (a) the pure CNTs electrode and (b) the CNTs-CNWs electrode in GBL ion solution as the electrolyte. The scan rate ranges from 50 mV/s to 1 V/s.....	122
Figure 5.12	Nyquist plots of two electrodes, performed at the frequency ranging from 1 to 10 ⁵ Hz. Pure CNTs electrode was denoted by ▲ and CNTs-CNWs electrode by ○.....	123
Figure 5.13	Measurements of the durability of two electrodes performed at the scan rate of 100 mV/s. Pure CNTs electrode was denoted by ■ and CNTs-CNWs electrode by ●.....	123
Figure 5.14	Equivalent circuit for the simulation of the impedance spectra of the capacitor cells shown in Figure 5.12.....	124